

# Studies of Touchdown Stability for Lunar Landing Vehicles

W. C. WALTON JR.,\* R. W. HERR,\* AND H. W. LEONARD†  
NASA Langley Research Center, Hampton, Va.

The paper presents early results of a study to establish practical procedures for predicting tumbling histories for a vehicle that impacts on a nonlevel surface. Symmetrical and asymmetrical inelastic impacts are discussed. Under the symmetrical case the main points of the simple theory are restated, critical modes of overturning for a four-legged body are identified, computed and experimental landing stability boundaries for a four-legged rigid model are correlated, and computed boundaries for two rigid configurations representative of current thinking about lunar landing vehicles are compared. Under asymmetrical impact there is a correlation of stability boundaries obtained experimentally and by digital simulation for the four-legged rigid model landing on a slope with vertical velocity only. It is found, interestingly, that asymmetrical approaches can be more critical than symmetrical approaches.

## Nomenclature

$g$	= acceleration due to gravity
$M$	= mass
$I$	= mass moment of inertia about center of gravity
$l$	= distance from center of gravity to the axis of the rotation produced by impact
$\bar{M}$	= dimensionless parameter = $ML^2/I$
$\beta$	= angle between the base plane of the vehicle and the perpendicular from the center of gravity to the axis of the rotation produced by impact
$\sigma$	= inclination of the landing surface
$V_f$	= forward approach velocity
$V_s$	= sink approach velocity
$\theta$	= angle between the vertical and the perpendicular from the center of gravity to the axis of the rotation produced by impact
$\alpha$	= pitch angle
$\lambda$	= angle of rotation about an axis through the initial impact point required to carry the vehicle from its orientation at initial impact to its orientation at second impact
$\dot{\gamma}$	= angular velocity just after impact about an axis through the point of impact
$\dot{\gamma}_{cr}$	= value of $\dot{\gamma}$ required to overturn the vehicle
$\dot{\rho}$	= angular velocity about an axis through the point of initial impact at the moment of impact
$X, Y, Z$	= coordinates of center of gravity in space-fixed system
$X_j, Y_j, Z_j$	= coordinates of $j$ th foot in space-fixed system
$C_{Xj}, C_{Yj}, C_{Zj}$	= viscous friction coefficients associated with $j$ th foot
$F_{Xj}, F_{Yj}, F_{Zj}$	= components of force on $j$ th foot in space-fixed system
$\xi, \eta, \zeta$	= coordinates in body-fixed system
$I_\xi, I_\eta, I_\zeta$	= principal moments of inertia
$\omega_\xi, \omega_\eta, \omega_\zeta$	= components of angular velocity in body-fixed system
$N_\xi, N_\eta, N_\zeta$	= components of torque in body-fixed system
$\phi, \psi, \theta$	= Euler angles

## Introduction

AMONG problems facing designers of lunar landing vehicles is that of assuring that the vehicle will not overturn even though the surface upon which it must land is as

Presented as Preprint 64-94 at the AIAA Aerospace Sciences Meeting, New York, January 20-22, 1964; revision received May 4, 1964.

\* Aerospace Technologist, Vibration and Dynamics Branch, Dynamics Loads Division.

† Aerospace Technologist, Vibration and Dynamics Branch, Dynamics Loads Division. Member AIAA.

yet effectively unknown. Rational evaluation of design with respect to this problem requires analysis of the tumbling motions that result when a rocket-propelled vehicle lands on an uneven surface.

Several organizations have studied lunar landing dynamics in recent years, generally relying upon dynamic model tests with supporting analyses. (See, for example, Refs. 1-6.) Analytical work has ranged from computing stability boundaries with the very simple inelastic impact theory to rather elaborate stability and loads studies based on computer programs, which account for the effects of shock absorber action and surface penetrability. Both the theoretical and the experimental work, however, have been largely restricted to symmetrical landings that result in two-dimensional tumbling motions.

This paper presents results of tests and analysis of the landing stability of a small rigid model, including both symmetrical and asymmetrical landings. The work was done as part of an effort currently under way to develop capability to predict stability during an asymmetrical landing. There is a review of two-dimensional inelastic impact theory and presentation of some experimental results that confirm this simple theory. Analytical and experimental results are also given which support the proposition that asymmetrical landings can impose more severe limitations on approach velocities than do symmetrical landings.

The work reported has been shaped to a considerable extent by anticipation of a configuration for the Apollo lunar excursion module (LEM) incorporating the ideas illustrated in Fig. 1. Propulsion units for descent from lunar orbit and relaunch into lunar orbit plus housing for the astronauts and the equipment necessary for their survival and work constitute the bulk of the central pod. The landing gear consists of four symmetrically attached legs terminating in foot pads.

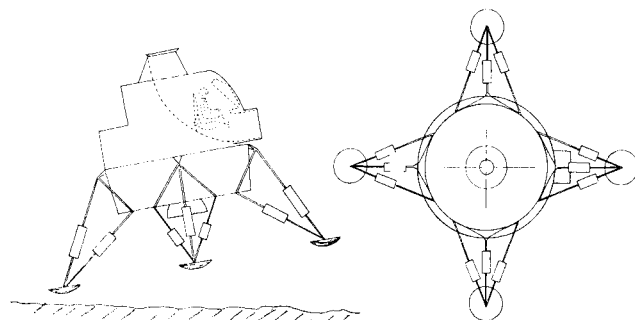


Fig. 1 Apollo lunar excursion module concept.

The legs are inverted tripods with tubular struts containing shock absorbers. The struts are attached to the pod by universal or swivel joints. Present thinking is that the pilot will attempt to land the LEM with one of its feet forward and that thrust will be terminated prior to contact with the lunar surface.

### Two-Dimensional Inelastic Impact Theory

The simplest theory available for the study of stability during landing is based on the following three assumptions:

- 1) The vehicle is a rigid body.
- 2) When a foot of the vehicle impinges upon the landing surface, impulsive forces are produced which immediately stop the foot. The vehicle thereafter rotates as though the foot were pinned unless another foot strikes, in which case the pin is released at the moment of the second impact.
- 3) Landing is two-dimensional in the sense that motion just prior to impact, the impulsive forces produced upon impact, and, consequently, the motion after impact are all symmetrical about a vertical plane through the center of gravity.

Under these assumptions, criteria for ascertaining whether or not a vehicle will overturn during landing are readily obtained by classical principles of mechanics. Referring to Fig. 2, suppose that the vehicle is rotating about an axis through a foot (or feet) stopped at point A with known angular velocity  $\dot{\gamma}$  in a direction that tends to carry the center of gravity over the axis of rotation. If the vehicle rotates from the position shown to the verge of toppling, which is when the center of gravity is directly over the axis of rotation, potential energy is gained. If the kinetic energy associated with  $\dot{\gamma}$  exceeds this change in potential energy, the vehicle will overturn. If the kinetic energy is the lesser of the two, rotation will stop short of the critical point, and the vehicle will fall back. Balancing the two energies gives for the critical angular velocity

$$\dot{\gamma}_{cr} = \left\{ \left( \frac{2g}{l} \right) [1 - \cos\theta] \frac{\bar{M}}{1 + \bar{M}} \right\}^{1/2} \quad (1)$$

where  $\bar{M} = MI^2/I$ .

Consider now that the vehicle has just struck the surface. Let the forward, sink, and pitch velocities just prior to impact be denoted  $V_f$ ,  $V_s$ , and  $\alpha$ , respectively. By representing the components of the forces which stop the foot as impulses, it may be shown that the angular velocity  $\dot{\gamma}$  resulting from the impact is

$$\dot{\gamma} = \{ \bar{M} [(V_f/l) \cos\theta - (V_s/l) \sin\theta] - \alpha \} / (1 + \bar{M}) \quad (2)$$

It is easily shown using Eq. (2) that, as would be expected, the vehicle loses kinetic energy as a result of the impact.

If, after the initial impact,  $\dot{\gamma}$  is less than  $\dot{\gamma}_{cr}$ , the vehicle will eventually strike upon a second foot (or pair of feet) and be shocked into rotation about a new axis. Let  $\lambda$  be the angle of rotation about the axis through A (the point of initial impact) required to carry the vehicle from its orientation at the initial impact to its orientation at the second impact. Then  $\dot{\rho}$ , the angular velocity about the axis through A at the moment of the second impact, is

$$\dot{\rho} = - \left\{ \dot{\gamma}^2 + \frac{(2g/l)\bar{M}[\cos\theta - \cos(\theta + \lambda)]}{(1 + \bar{M})} \right\}^{1/2} \quad (3)$$

Use of Eqs. (1-3) in proper sequences allows computation of stability boundaries as a function of approach conditions and the geometry of the landing surface for approaches leading to any mode of tumbling conforming to the assumptions previously stated. Shown in Fig. 3 are four such modes that may be termed critical in the following limited but useful sense: Let the landing surface be a slope that is planar except for irregularities that may be large enough to affect

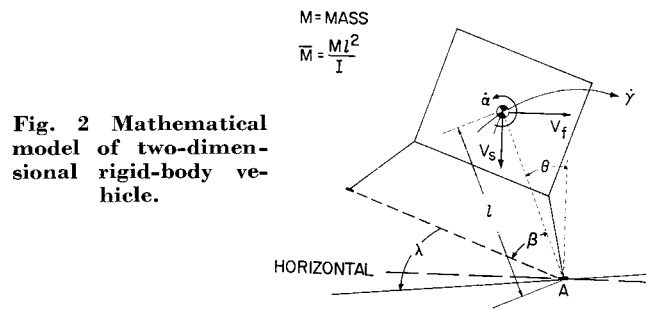


Fig. 2 Mathematical model of two-dimensional rigid-body vehicle.

the sequence of impacts of feet, but not large enough to substantially affect the landing site gradient. Then, given definite limits on the absolute magnitudes of the approach velocities, pitch rate, and pitch attitude, and on the gradient of the landing surface, if the vehicle is stable for approaches leading to these four modes of tumbling, then it is stable within the limits of two-dimensional inelastic impact theory. The nomenclature of these modes is derived from the number of feet which impact and the order in which the impacts occur:

- 1) Two and over: Two feet stick simultaneously; the vehicle then rotates about an axis connecting the two feet so as to carry the center of gravity over the axis of rotation.
- 2) Two-two and over: Two feet stick simultaneously; the vehicle then rotates leading to a two and over impact on the remaining two feet.
- 3) Two-one and over: Two feet stick simultaneously; the vehicle then rotates until a single other foot sticks. There is then a rotation about an axis through the single pinned foot carrying the center of gravity over the axis of rotation.
- 4) One-two-one and over: A single foot sticks; the vehicle then rotates about an axis through this foot leading to a two-one and over impact involving the remaining feet.

Proof that one need consider only these four modes under the conditions stated is quite straightforward with the use of Eqs. (1-3).

### Experimental Check on Impact Theory

One of the first objectives of the study was to test this simple method for computing stability boundaries under conditions compatible with the assumptions. The model (Fig. 4) was a solid aluminum block,  $3 \times 3 \times 4.5$  in. high with a sharp aluminum spike protruding downward about

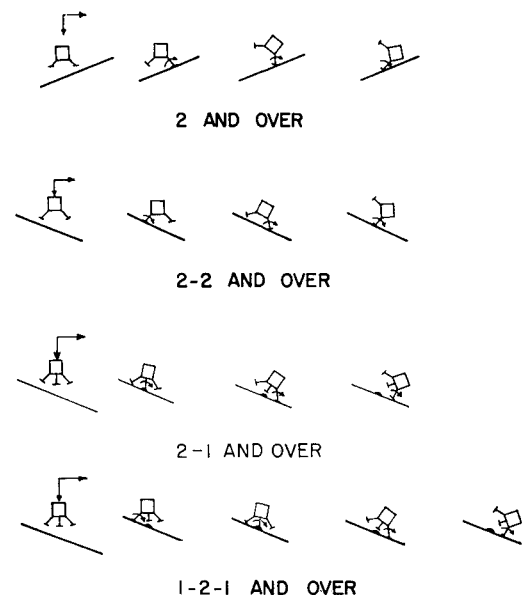


Fig. 3 Critical modes of two-dimensional tumbling.

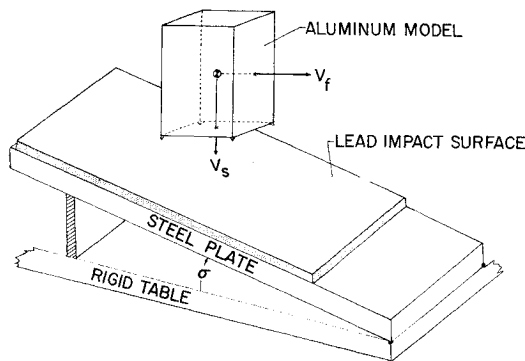


Fig. 4 Apparatus for rigid-body experiment.

$\frac{1}{16}$  in. from each corner of the base. The landing surface was a sheet of lead atop a heavy steel plate. The inclination of the surface  $\sigma$  was adjustable. Lead was selected as the landing surface for three reasons: 1) there was no perceptible rebound, 2) when a foot struck there was enough penetration to stop the foot abruptly, and 3) an impacted foot could lift easily upon subsequent impact of other feet. Prior attempts to construct landing surfaces of plywood and of hardwood proved unsatisfactory because of rebound.

Theory and experiment are compared in Fig. 5 for what is perhaps the simplest kind of two-dimensional tumble. The block starts from rest with two feet, designated for convenience the rear feet, planted on a sloping surface, and the other two feet, designated the front feet, raised off the surface. The block rotates about an axis through the rear feet until the front feet strike, which sets up a rotation about an axis through the front feet (a two-two and over mode with zero approach velocity);  $\alpha$  and  $\sigma$  are the only variables. The minimum inclination  $\sigma$  for which the vehicle will overturn is plotted against  $\alpha$ . Results from the theory and experiment agree quite well.

To obtain the data shown in Fig. 6, the block was swung as a pendulum and released at the lowest point of the swing to drop upon a level surface. The releases were with two feet forward, and the pitch rate was zero. For negative pitch, a two and over mode results; for positive pitch, a two-two and over mode results. The forward velocity required to overturn the block is plotted against pitch angle for each of four sink velocities. In addition to demonstrating reasonably good agreement between experiment and theory, the plots show a striking discontinuity in the stability boundary at  $\alpha = 0^\circ$  associated with the change in mode. The discontinuity is perfectly reasonable when one considers that sink velocity in the approach rocks the block back when the initial impact is on the front feet, but rocks it forward when the initial impact is on the rear feet. For the higher sink velocities a slightly nose-down approach is clearly desirable for stability. The relative advantage of a nose-down landing decreases, however, as the sink velocity is decreased.

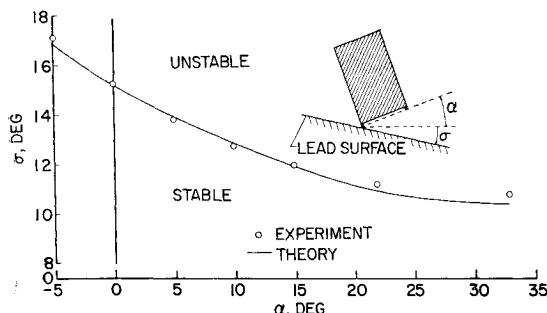


Fig. 5 Variation of surface inclination with pitch angle for neutral stability at zero approach velocities (2-2 and over mode).

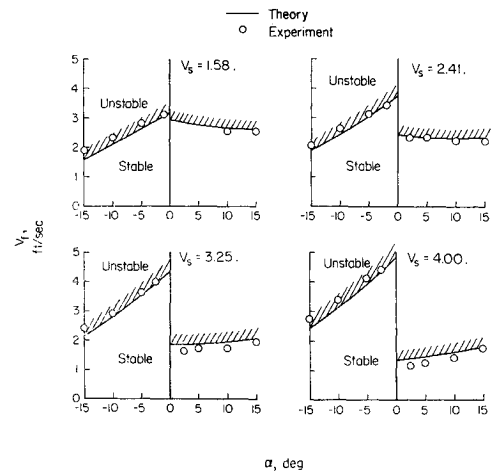


Fig. 6 Variation of forward velocity with pitch angle for neutral stability at various sink velocities.

### Trends for Representative Configurations

In order to obtain trends based on reasonably realistic structural parameters, two hypothetical four-legged configurations were sized to meet roughly the current requirements for a lunar landing vehicle. Some computed two-dimensional stability boundaries for the two configurations are shown in Figs. 7 and 8. Sink velocity is plotted against forward velocity for neutral stability in each of four modes of two-dimensional overturning. The numerical values of the parameters used in the calculations are given in Table 1. The essential difference in the configurations is that configuration II has a substantially lower center of gravity, as comparison of the angles  $\beta$  will show. In consideration of the plan to land LEM with one foot forward, the one-two-one mode and the one-one mode are of special interest. (A one-one and over mode starts and ends like a one-two-one mode, but there is no impact on the center feet.) Although both configurations are extremely stable in a one-one mode, for configuration II, a one-two-one mode is less stable than a two-two mode. Since the possibility of an impact on the center feet must be considered, the relative advantages of one-foot-forward and two-feet-forward landings require examination. It is also noted that lowering the center of gravity improved stability in the two-two mode substantially, but in the one-two-one mode only moderately.

### Three-Dimensional Studies

The preceding theory and experiments have important limitations. They cannot account for the effects of shock-absorber action or of a penetrable surface, and perfect two-dimensional tumbling is unlikely in practice. Concerning the latter restriction, the authors are, at present, trying to determine whether the assumption of two-dimensional tumbling leads to conservative stability estimates. Although this work is not complete, the following results suggest that the assumption is not conservative.

Table 1 Parameters used for Figs. 7 and 8

	Configuration I, Fig. 7		Configuration II, Fig. 8	
	one-one; one-two-one	two; two-two	one-one; one-two-one	two; two-two
For modes				
$g/l \text{ sec}^{-2}$	0.270	0.310	0.306	0.364
$M = Ml^2/I$	18.0	13.5	13.9	9.83
$\beta$ , deg (see Fig. 2)	46.7	57.0	40.4	50.2

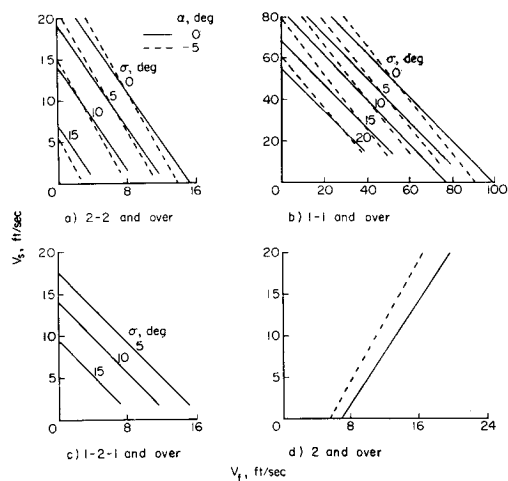


Fig. 7 Representative two-dimensional stability boundaries (configuration I).

Experiments

Using the same apparatus (Fig. 4), the block was dropped with no horizontal velocity, no pitch, and no pitch rate onto a sloping surface. A new variable, the yaw angle  $\psi$ , was introduced (Fig. 9). Figure 10 shows experimental values of the minimum surface inclination  $\sigma$  at which the block will overturn for  $V_s = 0$  and  $V_s = 3.25$  fps, and Fig. 11 shows experimental values of the minimum sink velocity  $V_s$  at which the block will overturn for  $\sigma = 10^\circ$ , all data being plotted against  $\psi$ .

Two-dimensional inelastic impact theory for a two-two mode is in good agreement with the experiments at  $\psi = 45^\circ$ , as would be expected. Ideally, two-dimensional tumbling would also be found for  $\psi = 0^\circ$ , but experimentally there were two difficulties with this case. First, it was hard to drop the block with sufficiently precise alignment to yield a two-dimensional tumble. The center of gravity would generally veer to one side rather than pass directly over the impacted downhill foot. The experimental values shown in Fig. 10 for  $\psi = 0^\circ$  correspond to tumbles obtained after many trials which appeared to the eye to be both two-dimensional and marginally stable. In obtaining the data shown in Fig. 11, the attempt to obtain a two-dimensional tumble at  $\psi = 0^\circ$  was abandoned after several trials. The second difficulty was that when a two-dimensional tumble was obtained for  $\psi = 0^\circ$ , it could not be discerned whether, following the initial impact on foot one, there was a distinct impact on feet two and four followed by a separate impact on foot three, or whether the build-up of force on foot three began

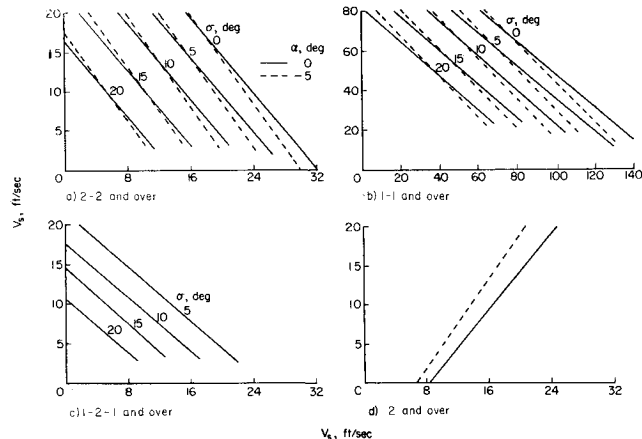


Fig. 8 Representative two-dimensional stability boundaries (configuration II).

before feet two and four were stopped. It was felt that, if the former case held, the experiment should be in agreement with the two-dimensional theory for a one-two-one mode and that, if the latter case held, the experiment should be higher than this theory. As shown (Fig. 10), the experimental critical  $\sigma$  at  $\psi = 0^\circ$  is slightly higher than the two-dimensional theory for  $V_s = 3.25$  fps and substantially higher for  $V_s = 0$ . This could be attributed to the fact that foot one penetrates the surface for the case of finite sink velocity, possibly making for a cleaner impact on the center feet.

For all three sets of data, stability boundaries at intermediate yaw angles drop below the end values given by experiment and/or two-dimensional theory. The lower curve in Fig. 10 and the curve in Fig. 11 show substantial drops in the boundaries, indicating that, for the rigid block, three-dimensional tumbling can impose more severe limitations on approach velocities than two-dimensional tumbling.

Theory

The second step taken in the development of procedures for the analysis of three-dimensional landing dynamics has been to drop the restriction requiring symmetrical ap-

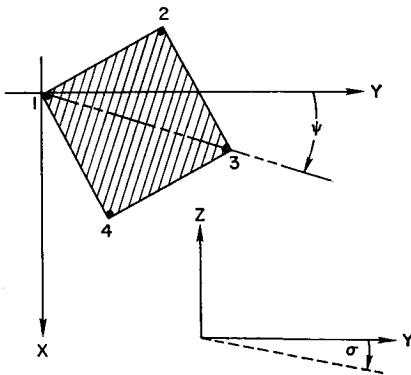


Fig. 9 Coordinate system for asymmetrical landings.

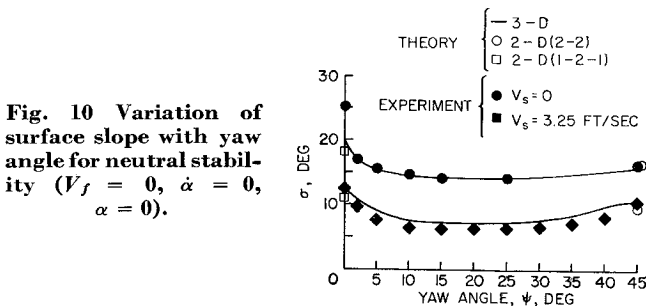


Fig. 10 Variation of surface slope with yaw angle for neutral stability ( $V_f = 0$ ,  $\alpha = 0$ ).

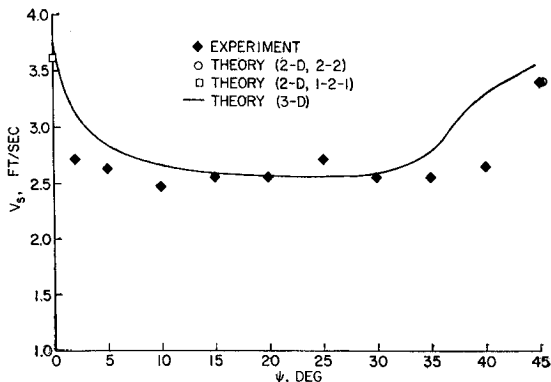


Fig. 11 Variation of sink velocity with yaw angle for neutral stability ( $\sigma = 10^\circ$ ,  $V_f = 0$ ,  $\alpha = 0$ ).

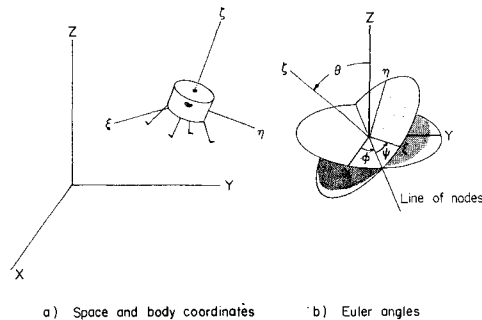


Fig. 12 Coordinate systems for three-dimensional analysis.

proaches, retaining, however, the assumptions that the vehicle is rigid and that a foot is stopped abruptly upon contact with the landing surface. Let there be, as shown in Fig. 12a, a space-fixed Cartesian coordinate system with axes  $X$ ,  $Y$ , and  $Z$  and a body-fixed cartesian system with axes  $\xi$ ,  $\eta$ , and  $\zeta$  along principal axes of the vehicle. Then the well-known equations of motion are

$$M\{\ddot{X}, \ddot{Y}, \ddot{Z}\} = \{F_X, F_Y, F_Z\} \quad (4)$$

$$I_\xi \dot{\omega}_\xi + (I_\zeta - I_\eta) \omega_\eta \omega_\zeta = N_\xi \quad (5a)$$

$$I_\eta \dot{\omega}_\eta + (I_\xi - I_\zeta) \omega_\xi \omega_\zeta = N_\eta \quad (5b)$$

$$I_\zeta \dot{\omega}_\zeta + (I_\eta - I_\xi) \omega_\xi \omega_\eta = N_\zeta \quad (5c)$$

The following auxiliary equations connect the components of the angular velocity vector with Euler angles (Fig. 12b) that describe the orientation of the vehicle with respect to the space-fixed axes:

$$\dot{\phi} = \frac{(\omega_\xi \sin \psi + \omega_\eta \cos \psi)}{\sin \theta} \quad (6a)$$

$$\dot{\theta} = \omega_\xi \cos \psi - \omega_\eta \sin \psi \quad (6b)$$

$$\dot{\psi} = \left[ \frac{(-\omega_\xi \cos \theta \sin \psi - \omega_\eta \cos \theta \cos \psi)}{\sin \theta} \right] + \omega_\zeta \quad (6c)$$

A digital-computer program has been devised to generate numerical solutions of the equations of motion. In the program, the forces are computed as follows: Forces other than gravitational forces are considered to act only at the feet. An arbitrary plane in the space-fixed system is designated the landing surface plane. The components of force on the  $j$ th foot,  $F_{Xj}$ ,  $F_{Yj}$ ,  $F_{Zj}$ , are set equal to zero if the foot is above the surface plane or if the foot is on or beneath the surface plane and  $\dot{Z}_j > 0$ . If the foot is on or beneath the surface plane and  $\dot{Z}_j \leq 0$ , the forces are computed by the equation

$$\{F_{Xj}, F_{Yj}, F_{Zj}\} = -\{C_{Xj}\dot{X}_j, C_{Yj}\dot{Y}_j, C_{Zj}\dot{Z}_j\} \quad (7)$$

where  $C_{Xj}$ , etc., are constants that may be arbitrarily assigned. Use of Eq. (7) amounts to saying that the surface is

like a viscous damper resisting the progress of a foot. This scheme for computing forces is not set forth as an ideal method of representing the landing surface when studies involving sliding and penetration of feet are an objective. It is, however, simple and has proved satisfactory for the present study, since a foot can be stopped by setting the viscous constants sufficiently high; yet there is little resistance to lifting of a foot if the space axes are oriented so that the  $Z$  axis is normal or nearly normal to the landing surface plane. At one time the authors were allowing forces along the  $X$  and  $Y$  axes to act whenever a foot was on or beneath the landing surface plane rather than nulling all forces on a foot the moment it begins to rise, as is done here. It was found, with that procedure, that substantial forces resisting lifting of a foot could develop, producing an unwanted stabilizing effect, if the  $Z$  axis was not perfectly normal to the landing surface.

The curves labeled 3-D theory in Figs. 11 and 12 were computed using the program with  $C_{Xj}$ ,  $C_{Yj}$ , and  $C_{Zj}$ , all set equal to 70 lb-sec/ft. For this value of viscosity, a foot upon crossing the surface was slowed, for all practical purposes, to a standstill before traveling  $\frac{1}{8}$  of an inch in any direction. The  $Z$  axis was taken vertical, not normal, to the landing surface.

The three-dimensional theory is in substantial agreement with the experiments and the two-dimensional theory, confirming the loss of stability associated with three-dimensional tumbling.

## Conclusions

For landings of a small, rigid, four-legged body where the feet are abruptly stopped: 1) the inelastic-impact theory gives reasonably accurate stability boundaries for two-dimensional tumbling; and 2) three-dimensional tumbling imposes more severe limitations on approach conditions for vertical landings than does two-dimensional tumbling.

## References

- Alper, J. R., "Landing dynamics; a survey of STL state-of-the-art and recommendations for further investigations," EM 13-5, 9758-6001-RU-000, Space Technology Lab., Inc. (January 1963).
- "Apollo LEM; touchdown systems studies and proposed development program," Rept. SPP-62-102, Bendix Products Aerospace Div. (October 1962).
- Sala, R., "Plan for the LEM landing gear stability drop tests," Rept. LTP-S60-1, Contract NAS 9-1100, Grumman Aircraft Engineering Corp. (April 1963).
- Blanchard, U. J., "Characteristics of a lunar landing configuration having various multiple leg landing gear arrangements," NASA TN D-2027 (1963).
- Donroe, F., "Results of landing gear stability drop tests  $\frac{1}{8}$  scale model LEM," Contract NAS 9-1100, Rept. LTR 904-16001, Grumman Aircraft Engineering Corp. (January 1963).
- Black, R. J., "Quadrupedal landing gear systems for spacecraft," J. Spacecraft Rockets 1, 196-203 (March-April 1964).